Challenges for density functional theory in simulating metal-metal singlet bonding: a case study of dimerized VO₂

Yubo Zhang^{1,*}, Da Ke¹, Junxiong Wu¹, Chutong Zhang¹, Lin Hou⁶, Baichen Lin^{2,3}, Zuhuang Chen^{4,5}, John P. Perdew⁶, Jianwei Sun^{6,*}

¹Minjiang Collaborative Center for Theoretical Physics, College of Physics and Electronic Information Engineering, Minjiang University, Fuzhou, China

²School of Materials Science and Engineering, Nanyang Technological University, Singapore, 639798, Republic of Singapore

³Institute of Materials Research and Engineering (IMRE), Agency for Science, Technology and Research (A*STAR), Singapore 138634,

Republic of Singapore

⁴School of Materials Science and Engineering, Harbin Institute of Technology, Shenzhen, Shenzhen 518055, China ⁵Flexible Printed Electronics Technology Center, Harbin Institute of Technology, Shenzhen, Shenzhen 518055, China ⁶Department of Physics and Engineering Physics, Tulane University, New Orleans, Louisiana 70118, USA

Corresponding emails: yubo.drzhang@mju.edu.cn, jsun@tulane.edu

VO₂ is renowned for its electric transition from an insulating monoclinic (M₁) phase characterized by V-V dimerized structures, to a metallic rutile (R) phase above 340 Kelvin. This transition is accompanied by a magnetic change: the M₁ phase exhibits a nonmagnetic spin-singlet state, while the R phase exhibits a state with local magnetic moments. Simultaneous simulation of the structural, electric, and magnetic properties of this compound is of fundamental importance, but the M₁ phase alone has posed a significant challenge to density functional theory (DFT). In this study, we show none of the commonly used DFT functionals, including those combined with on-site Hubbard U to better treat 3d electrons, can accurately predict the V-V dimer length. The spin-restricted method tends to overestimate the strength of the V-V bonds, resulting in a small V-V bond length. Conversely, the spin-symmetry-breaking method exhibits the opposite trends. Each of these two bond-calculation methods underscores one of the two contentious mechanisms, i.e., Peierls lattice distortion or Mott localization due to electron-electron repulsion, involved in the metal-insulator transition in VO2. To elucidate the challenges encountered in DFT, we also employ an effective Hamiltonian that integrates one-dimensional magnetic sites, thereby revealing the inherent difficulties linked with the DFT computations.

Keywords: Dimerized VO₂, Singlet bonding, r²SCAN, Spin Symmetry breaking

1. Introduction

In transition-metal compounds, the coupling between the lattice-charge-spin-orbital degree of freedom makes these materials a fascinating playground for developing multiple functionalities [1]. At the microscopic level, these interesting properties originate from or are associated with correlated electrons in the d or f orbitals. For a long time, the simulation of these materials has been considered to be a grand challenge for the Kohn-Sham density functional theory (DFT) [2], the workhorse of the material study, and there is a prevalent belief that DFT is a mean-field theory incapable of describing the correlated d- and f-electron systems. One canonical example is the DFT's inability to predict the insulating behavior of NiO solid [3] using the local-density approximation (LDA) [2,4]. Subsequently, introducing a Hubbard U correction onto the Ni-3d orbitals largely resolves the problem. This fact strengthens the belief that electronic correlation is beyond the scope of the DFT approaches.

However, recent advancements show that the DFT approaches can simulate more and more complex materials with *d*- and *f*- electrons. Most noticeably, combining the SCAN (strongly-constrained and appropriately normed) functional [5] with the spin-symmetry-breaking (SSB) technique [6], but without the empirical Hubbard *U* parameter, we have reliably reproduced many Mott-like characteristics of the prototypical correlated materials, such as FeO and cuprates [7,8,9]. For example, SCAN opens a bandgap for FeO not only in the antiferromagnetic (AFM) model, which has a long-range magnetic order but also in the disordered-local-moment (DLM) model that does not rely on magnetic ordering [7]. Similar predictions have been made in the un-doped cuprates like LaCu₂O₄ [8] and hole-doped YBa₂Cu₃O₇ [9], a group of well-known correlated materials. Moreover, Perdew et al. [6] recently pointed out that "the spin-symmetry-breaking can reveal strong correlations among the electrons that are present in a symmetry-unbroken wavefunction" if the broken symmetry persists for a long time. This is usually true for the conventional Mott insulators. For example, according to Philip Anderson [10], the spin-flip span in the AFM solid NiO is typically three years, much longer than the duration of any experimental measurement (e.g., neutron scattering) [6]. These arguments may lay the foundation that the broken symmetry "may correspond to an actual state" in condensed matter, as pointed out by Martin, Reining, and Ceperley [11].

Besides the antiferromagnets with spatially *extended* geometries (such as NiO and FeO), a particular class of solids contains *isolated* motifs formed by transition metal-metal bonds [12,13,14]. For example, two and three V atoms form relatively isolated trimer and dimer motifs in LiVO₂ [15] and VO₂ [16], respectively. In the isolated motifs, the inter-site AFM coupling is quite strong, and the spin interactions are maximally entangled among the sites, which leads to the spin-singlet bonding state. The metal-metal interaction in some solid compounds could be so strong that the transition-metal atoms form "*metallic clusters*" and "*molecules in solids*" [12,13,14], leading to a bond length comparable with or even shorter than that of the elemental metals. The shortest V-V bonds are 2.62 Å in VO₂ [16] and 2.56 Å in LiVO₂ [17], compared with 2.629 Å [18] in the vanadium metal.

The metal-metal singlet bonding state is characterized by intense spin fluctuations and is observed to be non-magnetic (also referred to as paramagnetic) in experiments. For the application of Kohn-Sham DFT, one can choose between spin-restricted and SSB simulation approaches. The spin-restricted method may be favored by some due to its superior alignment with the non-magnetic reality. However, others might argue that the transition-metal 3d orbitals inherently localize to form a local magnetic moment, suggesting the SSB method, as underscored by Perdew et al., could be more "revealing" [6]. The suitability of these methods for the spin-singlet state remains ambiguous at this juncture. Complexity in describing the spin-singlet state and related magnetism can be increased when considering the recent findings of Streltsov and Khomskii, who noted that "strong intersite coupling may invalidate the standard single-site starting point for considering magnetism" [19].

In this work, we select VO_2 as an example to evaluate the applicability of Kohn-Sham DFT approaches, including various exchange-correlation functionals on the first four rungs of Jacob's ladder of DFT [20]. VO_2 is a fascinating material having three simultaneous transitions around room temperature [21], i.e., (1) the structural transition from the dimerized monoclinic (referred to as M_1) phase to the high-temperature rutile (referred to as R) phase, where the dimers break apart, (2) the associated transition of electric transport behaviors from an insulator to a metal, (3) the magnetic transition from a non-magnetic M_1 phase to a state with local magnetic moments in R. The concurrent simulation of structural, electrical, and magnetic properties is of utmost importance. Yet, prior DFT research has faced considerable challenges and ambiguity in choosing suitable structural and magnetic models, exchange-correlation functionals, and Hubbard U parameters [21]. There have been instances where researchers confidently predict specific properties while overlooking conflicting outcomes. A particularly perplexing issue pertains to reconciling two ostensibly contradictory properties observed in the $M_1 VO_2$: the lack of net magnetic moments and

the tendency to develop local magnetism. Addressing this paradox is vital for understanding the driving force of insulator-metal transition, which is still debatable [21] among the Peierls, Mott, or Peierls-Mott-collaborative mechanisms starting from the early days by Goodenough [22].

We close this introduction with a discussion of how correlation is included in a theory that in practice computes only a non-interacting wavefunction. Kohn-Sham DFT is a computationally efficient and thus widely-used simplification of the quantum mechanics of electronic ground states. It has an underlying exact theory [2,23] in which the exact exchange-correlation energy for a given electron density is defined [23] by a search over correlated wavefunctions constrained to have that electron density. This underlying exact theory would yield the exact groundstate energy and electron density for any system of interacting electrons in the presence of an external scalar potential, with the help of an auxiliary non-interacting or single-determinant wavefunction that yields the noninteracting part of the kinetic energy and is not intended to be an approximation to the true correlated wavefunction. There is little doubt that this underlying exact theory applies even to strongly-correlated systems. The exact manybody exchange-correlation energy has about 20 known mathematical properties [24] which can be built into its practical approximations. The approximations also rely on appropriate norms [24], such as the electron gas of uniform density, rare-gas atoms, etc., all of which are normally correlated. Nevertheless, a good non-empirical approximation plus energy-minimizing symmetry breaking can often predict and describe the energetic effects of strong correlation on real materials [6,7,8,9,25,26]. Strong correlation can arise from degeneracies or neardegeneracies of the exact Kohn-Sham non-interacting system. Breaking the symmetry can break the degeneracy and transform strong correlation into normal correlation that a good approximate functional can handle.

There is of course no guarantee that any particular approximate density functional can accurately describe the energetic effects of strong correlation through symmetry breaking. Numerical evidence suggests that functionals from the simplest (local spin density) approximation [25] to SCAN or r²SCAN [7] can do so for the simple case of stretched H₂. For the more complex case of equilibrium singlet C₂, accuracy improves dramatically through the same sequence of improving functionals [26]. For the even more complex *d* and *f* materials, SCAN plus symmetry breaking is sometimes but not always accurate, and further-improved functionals appear to be needed. A density functional approximation that can deal with strong correlation and still preserve symmetry must in all probability make use of some unoccupied orbitals [27].

The SCAN approximate functional [5] was constructed to satisfy 17 exact constraints, without any fitting to bonded systems, but it is not exact for all one-electron densities. Work on a proper self-interaction correction to SCAN is ongoing [28,29], but for now SCAN plus symmetry breaking describes the effects of strong correlation in only some systems. In other systems, SCAN can still be supplemented with a (usually empirical) +U correction that mimics [30] some of the effects of self-interaction correction.

Stationary states have time-dependent correlations between density fluctuations that can be extracted from the wavefunction with the help of a product of position- and time-dependent one-particle density operators. As the size of a system grows, the frequencies of these fluctuations can drop toward zero and freeze out in the one-particle density. In infinite systems, the symmetry-unbroken ground-state wavefunction can become degenerate with observable symmetry-broken wavefunctions. In density functional theory, symmetry breaking can often indicate [6] the nature of the slow density fluctuations or strong correlations. For example, a singlet state can show strong antiferromagnetic correlations [31].

Since "correlation" means the effect of Coulomb interaction on the electron pair density or equivalently on the exchange-correlation hole around an electron, can we see this within DFT without a correlated wavefunction? The

exchange-correlation energy itself is just an integral over the system-averaged exchange-correlation hole [25,32], which is modelled in the construction of some approximate functionals like PBE [33,34] and can be reverse-engineered for others like SCAN. Spin symmetry breaking can, like strong correlation, make the hole deeper and more short-ranged [35]. Correlation is real, and DFT can deal effectively with strong correlation, exactly in principle and (at least in many cases) approximately in practice.

2. Computational details

Most simulations are carried out using the r²SCAN functional [36], which is a revised form of the original SCAN meta-GGA [5], as implemented in the VASP code [37,38]. Both r²SCAN and SCAN are general-purpose functionals on the third rung of Jacob's ladder, yet the former improves the numerical stability significantly. For comparison, we also use other density functionals, including the first rung LDA [4], the second rung generalized-gradient-approximation (GGA) in the form of Perdew-Burke-Ernzerhof (PBE) [33], and the range-separated hybrid functional of Heyd-Scuseria-Ernzerhof (HSE06) [39,40] on the fourth rung. The Heisenberg-type spin exchange parameters, *J*, are extracted using the LKAG method implemented in the TB2J code [41,42]. The chemical bonding property is quantitatively analyzed via the *projected Crystal-Orbital-Hamilton-Population* (pCOHP) [43,44] as implemented in the Lobster code [45]. We find that the effects of spin-orbit coupling play a minor role in the studied properties, and we exclude them from this work. By default, the crystal structures are completely relaxed unless specified otherwise.

3. Results and Discussions

3.1. Insulating band structure and V-V dimer length

Given that the experimentally observed dimerized M_1 phase is a non-magnetic insulator, a key criterion for validating a DFT simulation is the successful reproduction of a gapped band structure, yet without any macroscopic magnetism. This requirement is met by the three theoretical models illustrated in Figure 1. Figure 1(a) represents the non-magnetic (NM) model, where spin-up and spin-down electrons are uniformly balanced across the entire structure. The band structure develops a gap of 0.277 eV [Figure 1(e)] according to the r²SCAN calculation, although it is underestimated compared with an experimentally measured optical bandgap of about 0.6 eV [16]. In the NM model, the emergence of a bandgap underscores the critical role of V-V dimerization. Two V-3d $d_{x^2-y^2}$ electrons strongly hybridize at the center of two V atomic sites, resulting in a dimerization distortion, a critical factor in the Peierls gapping mechanism [46]. The bonding characteristics will be visualized in Section 3.3.

Restricting the spin polarization could be an aggressive hypothesis since the V-3d electrons are intrinsically localized. A circumvention is to allow spin polarization and simultaneously assign an AFM spin configuration to nullify the overall magnetism. This technique is known as SSB for DFT [6,11], and the model is shown in Figure 1(b). The calculated local magnetic moment is 0.96 μ_B , and the bandgap is 0.287 eV [Figure 1(f)]. The gapping is due to the well-known Mott mechanism, which states that double electron occupation of a single atomic site (and thus inter-site electron hopping) is prevented due to significant on-site Coulombic repulsion [3]. Moreover, SSB leads to considerable energy lowering, as established previously [6]. Here, the AFM model is more stable than the NM model by 112.2 meV/formula [Figure 1(d)].

The long-range magnetic ordering in the AFM model, absent in experiments, can be further removed using the disordered-local-moment (DLM) model Figure 1(c). Note that the DLM superstructure keeps the AFM pattern within each V-V dimer, which is favored energetically to be discussed in Figure 3, but introduces a disordering pattern between the dimers. The DLM model, without a long-range magnetic ordering, is energetically almost degenerate with the AFM model and has a similar bandgap [Figure 1(d,g)].

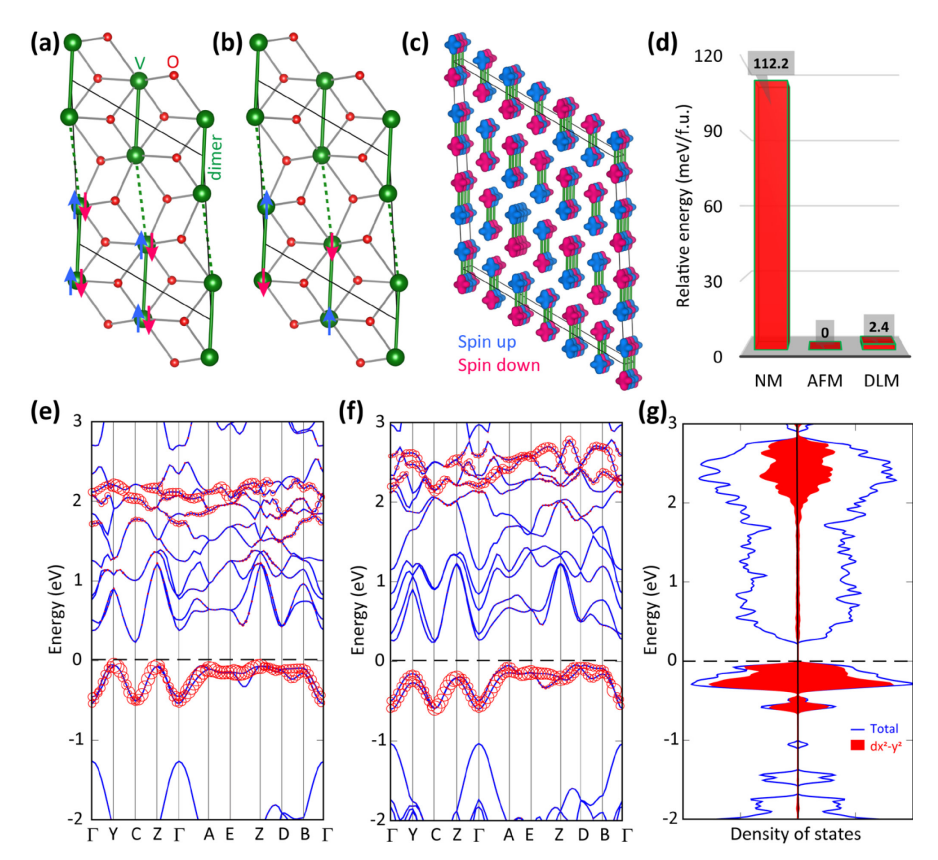


Figure 1. Three theoretical models yielding insulating states of M_1 VO₂ without producing macroscopic magnetism. (a) Spin-restricted non-magnetic (NM) state. The V-V intra- and inter-dimer bonds are denoted as solid and dashed green lines. (b) Each V site is spin-polarized and exhibits antiferromagnetic (AFM) coupling with neighboring sites. (c) Antiferromagnetic coupling within V-V dimers, but the magnetic coupling between different dimers is disordered (i.e., disordered-local-moment, DLM). (d) Relative energies of three models. (e,f,g) Corresponding band structures or density-of-states, with the characteristics of $d_{\chi^2-y^2}$ orbitals highlighted in red. The dashed lines indicate the valence band maximum.

Since both the spin-restricted and SSB methods yield bandgaps, further evaluations, such as those involving crystal structures, become necessary. As shown in Figure 2(a), predicting the V-V dimer length is a challenging task, contrasting with the relatively straightforward prediction of insulating band structures. We conduct comparative studies using four functionals: LDA, PBE, r²SCAN, and HSE06. Besides the spin-restricted NM state, we consider SSB states in two forms: AFM and ferromagnetic (FM) spin configurations. Interestingly, all predicted dimer lengths deviate noticeably from the experimental value of 2.62 Å [16], being either too short or excessively long. An analysis of the magnetic moment [Figure 2(b)] discloses a clear connection: the dimer length is markedly underestimated when the V's magnetic moment is absent, but overestimated once the magnetic moment is stabilized. For instance, in all calculations, LDA cannot stabilize local magnetic moments for V atoms and consistently underestimates the dimer length. PBE cannot stabilize the SSB-AFM model, which eventually converges to the NM state. PBE results in extremely short dimer lengths in the NM state, whereas in the SSB-FM model, which stabilizes local magnetic moments for V atoms, the dimer lengths generated by PBE are too long. The behaviors of r²SCAN and HSE06 are qualitatively alike: the dimer length is even shorter in the NM calculations where local magnetic moments are absent, but excessively long when the moments are stabilized.

Previous studies have established that the SCAN and r²SCAN functionals are generally reliable in describing the geometries of numerous materials [47,48], and noticeable deviations arise in correlated materials due to the

persistence of the self-interaction error [49,50]. To mitigate this error in VO₂, we combine the r^2SCAN functional with the on-site Hubbard U correction ($r^2SCAN+U$) to reevaluate the structural and magnetic properties using the SSB-AFM model. Interestingly, the V-V intra-dimer length increases with higher values of U [Figure 2(d)], while the distance between dimers decreases accordingly. The dimer structure is wholly disrupted when U reaches 2.0 eV, collapsing into the R phase with equally distributed V ions. Furthermore, a nearly linear correlation exists between the dimer length and the local magnetic moment [Figure 2(e)], indicating that the magnetic moment destabilizes the dimer structure.

Another unexpected result is the stability of the FM spin configuration calculated by the PBE and r^2SCAN functionals, which disagrees with experiments [Figure 2(c)]. The reason will be explained later.

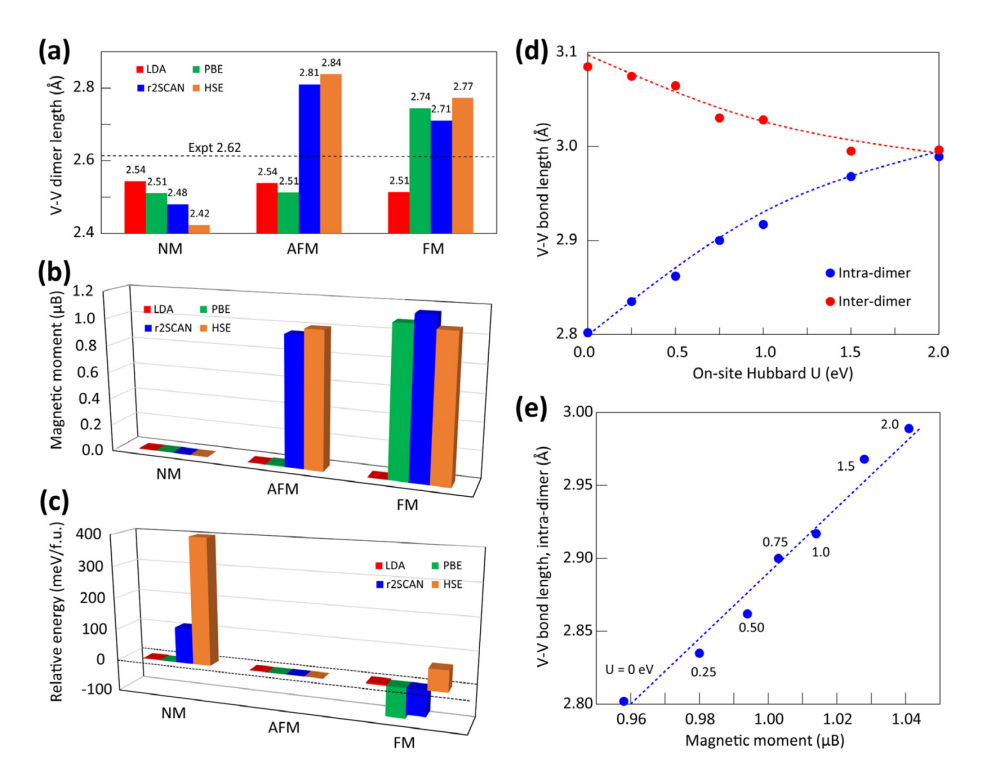


Figure 2. Structural, energetic, and magnetic properties of M_1 VO₂. (a) V-V intra-dimer bond length. Simulations are done with LDA, PBE-GGA, r^2 SCAN meta-GGA, and HSE06 hybrid functionals, in combination with spin-restricted NM and the SSB-AFM/FM. (b) Local magnetic moments of V ions. (c) Relative energies of the NM/FM models with respect to the AFM model. (d) V-V bond length from the r^2 SCAN+U simulations as a function of Hubbard U. (e) V-V intra-dimer length plotted against the local magnetic moments of V ions. Note that the subplots (d,e) are based on the SSB-AFM model.

The preceding evaluations make it clear that spin-restricted calculations utilizing diverse density functionals tend to consistently undervalue the dimer length, which might be attributed to the missing strong correlation. The SSB method is capable of capturing a substantial part of these correlation effects [6], leading to a notable reduction in energy compared to the NM state. However, this SSB method brings forth two new complications in $M_1 \text{ VO}_2$: it destabilizes the dimer structure due to the emergence of local magnetic moments, and (except in HSE) it indicates the FM spin configuration as the most stable. Additionally, it is crucial to note that applying on-site Hubbard U to the SSB model exacerbates the dimer length problem. These findings hint that the issues may extend beyond the tested functionals. The following sections examine a potential factor contributing to these difficulties.

3.2. Instability of Néel-ordered or local-moment state against valence-bond state

In the framework of the SSB-AFM model utilized for DFT simulations, each spin is situated on a discrete atomic site, with their interactions taken into account subsequently. This way of treating spin interactions aligns with the principles of the Mott insulating mechanism, which emphasizes the electronic repulsion among the spin sites. The magnetic ground state is recognized as the Néel state for traditional three-dimensional solids such as NiO and FeO. However, Sachdev et al. [51,52] have established that the *Néel-ordered* state is not the ground state for low-dimensional antiferromagnets due to its instability, which prompts a transition into a *valence-bond state* that highlights enhanced spin interactions within the low-dimensional motifs. In the case of M₁ VO₂, the V-V dimers structurally resemble zero-dimensional "molecules". These earlier investigations on the valence-bond state, employing the effective Hamiltonian method, can provide valuable insights into understanding the challenges faced by DFT, suggesting a relationship between the zero-dimensional characteristic of the V-V dimers and the spin interactions within VO₂.

We substantiate the above arguments by extracting the spin interaction parameters in VO₂, as shown in Figure 3. The central V₀ atom is surrounded by ten neighboring atoms, where the V₁ and V₂ atoms are in line along the dimer chain (the y direction), and the remaining eight are situated off the chain. We first focus on the J parameters for the experimental crystal structure. Notably, the intra-dimer exchange interaction is remarkably strong ($J_{V_0-V_1} = -49.2$ meV), making the other interactions ($J_{V_0-V_2}$ and $J_{V_0-V_x}$ with $x \ge 3$) essentially negligible. Therefore, the strong intra-dimer AFM spin interactions define the zero-dimensional structural motifs, i.e., the V-V dimers. Structural relaxation leads to a significant reduction of the intra-dimer spin interaction to a value of $J_{V_0-V_1} = -15.9$ meV. This reduction aligns with the observed increase in the dimer length [Figure 2(a)]. As the structure relaxes further, the intra-dimer interaction $J_{V_0-V_1}$ begins to converge with the inter-dimer interaction $J_{V_0-V_2}$. When V-V dimerization entirely disappears in the limit, the magnetic ions form a one-dimensional spin chain.

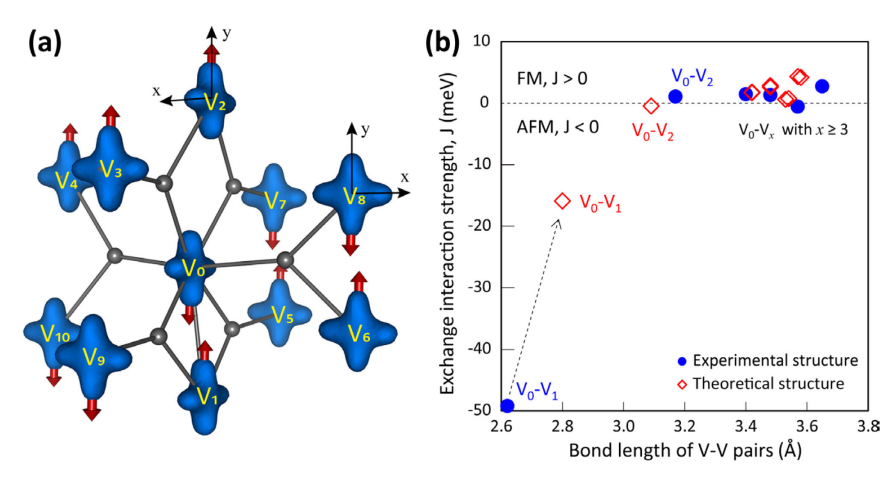


Figure 3. Spin interactions in the M_1 VO₂. (a) Crystal structures showing the central V₀ atom and its ten neighbors. The red arrows denote the assumed AFM spin configuration in the simulation. The blue isosurfaces are the electron density of the polarized $d_{x^2-y^2}$ orbitals [53], whose local coordinates are defined by black arrows. (b) Spin exchange parameters extracted from the SSB-AFM model. Two geometries, i.e., the experimental and r²SCAN-relaxed crystal structures, are used in calculations. Here, V₀ and V₁ form a dimer.

The comparative stability of the Néel-ordered and valence-bond states can be illustrated using a one-dimensional illustrative model, as depicted schematically in Figure 4, reproduced from Reference [1]. The instability of one-dimensional spin chains is referred to as the Spin-Peierls problem, which suggests that equally distributed AFM spins within a one-dimensional chain are unstable against spin pairing. The uniformly distributed spins, i.e.,

the Néel-ordered state, are characterized by an exchange energy:

$$E^{\text{N\'eel-ordered}} = NJ\langle \mathbf{S}_i \cdot \mathbf{S}_j \rangle = NJ\langle S_i^z S_j^z \rangle = NJ(-\frac{1}{4}) = -\frac{1}{4}NJ. \tag{1}$$

Here, N represents the number of magnetic interactions, and J represents the exchange strength. Only the z-component of spin, S^z , contributes to this energy. Contrastingly, spin pairing leads to a *valence-bond state*, and the associated spin interaction energy is:

$$E^{\text{Valence-bond}} = \frac{N}{2} J' \langle \mathbf{S}_i \cdot \mathbf{S}_j \rangle = \frac{N}{2} J' \langle S_i^{x} S_j^{x} + S_i^{y} S_j^{y} + S_i^{z} S_j^{z} \rangle = \frac{N}{2} J' (-\frac{3}{4}) = -\frac{3}{8} N J'.$$
 (2)

In this case, the inter-dimer exchange becomes negligible, causing the valence-bond state to lose half of the spin interactions. However, the valence-bond state could be more stable, because the spin is isotropic and all three spin components contribute equally. It requires that $J' > \frac{2}{3}J$, which is generally true as the exchange interaction strengthens after dimerization [see the example of VO₂ in Figure 3(b)].

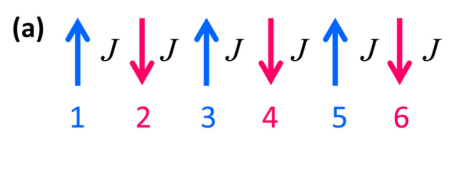


Figure 4. Spin-Peierls transition in the one-dimensional spin chain with AFM coupling, reproduced from [1]. (a) Néel-ordered state with uniformly distributed spins. The inter-site exchange parameter is J. (b) Valence-bond state with dimer structures. The exchange strength within a dimer is J', while the inter-dimer magnetic interaction is neglectable.

The emergence of the valence-bond state highlights the significance of spin entanglement, a key physical principle intrinsic to many quantum materials [54]. For example, $TICuCl_3$ [55] and $RuCl_3$ [56] exhibit a quantum phase transition from the Néel-ordered phase to a quantum-disordered phase under external pressure. This disordered phase is predominantly characterized by the valence-bond state. Turning our attention back to M_1 VO₂, each V⁴⁺ ion in the V-V dimer motif carries one valence electron, causing the motif to behave akin to a two-electron system. It would be more appropriate to consider VO₂ as a *valence-bond solid* [1] because there is no spin interaction between dimers as shown in Figure 3(b).

3.3. Description of two-electron singlet bonding by Kohn-Sham DFT

Is there any reason preventing the DFT from accurately describing the valence-bond state in M_1 VO₂? Since Kohn-Sham DFT is formulated in terms of the Kohn-Sham molecular orbitals, it is informative to express the two-electron wave function. The molecular-orbital theory (MOT), pioneered by Mulliken and Hund in the late 1920s [57,58,59,60,61], defines the spin-singlet state of a valence bond in the independent-electron (IE) representation as [62]:

$$\Psi_{\text{MOT,IE}}^{Singlet} = \frac{1}{2\sqrt{1+S_{1,2}}} [\varphi_1(\mathbf{r}_1)\varphi_2(\mathbf{r}_2) + \varphi_2(\mathbf{r}_1)\varphi_1(\mathbf{r}_2)] [\alpha_1\beta_2 - \beta_1\alpha_2]$$

$$+ \frac{1}{2\sqrt{1+S_{1,2}}} [\varphi_1(\mathbf{r}_1)\varphi_1(\mathbf{r}_2) + \varphi_2(\mathbf{r}_1)\varphi_2(\mathbf{r}_2)] [\alpha_1\beta_2 - \beta_1\alpha_2] .$$
(3)

Here, $\varphi(r)$ represents the one-electron atomic wave function, and the double overlap integral is denoted as

 $S_{1,2} = \langle \varphi_1(r_1)\varphi_2(r_2)|\varphi_1(r_2)\varphi_2(r_1)\rangle$. α and β are the spin functions. However, a potential issue may arise in $\Psi_{\text{MOT,IE}}^{Singlet}$. The two ionic terms $\varphi_1(r_1)\varphi_1(r_2) + \varphi_2(r_1)\varphi_2(r_2)$, representing a single atomic site occupied by two electrons, appears at an equally high probability as the other terms. This situation can result in unphysical Coulombic repulsion. While this repulsion is less critical for delocalized electrons (as observed in the H₂ molecule with an equilibrium geometry), it becomes particularly prominent in the presence of localized electrons, such as V-3d electrons in VO₂.

Given these insights, we can explain the discrepancy in calculating the V-V dimer length between the spin-restricted and SSB models. The V-V bond length is determined by a delicate balance between two interactions. On one side, there is an attractive covalent bonding between neighboring V $d_{x^2-y^2}$ orbitals in a spin-singlet state. This bonding promotes electron overlap around the bond center, resulting in a shortened V-V bond. Conversely, the localization of V-3d orbitals favors spatial separation of the individual V atoms, leading to charge depletion at the bond center and a consequent elongation of the bond length. In the spin-restricted calculation, the suppression of electron localization results in a bias towards covalence, favoring a bond length shorter than the experimental value. Alternatively, the spin polarization of V-3d orbitals in the SSB model better captures the electronic correlation, which localizes d electrons. This however overestimates ionic characteristic interactions within a V-V dimer. As a result, this overestimation contributes to a longer bond length than the experimental data.

Our arguments are corroborated by examining the chemical bonding properties using the projected-Crystal-Orbital-Hamilton-Population (pCOHP) approach [43,44]. Figure 5(a) visualizes the bonding interactions between two V-V atoms in a dimer, where the interaction of five d orbitals or solely the $d_{x^2-y^2}$ orbital is represented by red shades or blue lines, respectively. It is the $d_{x^2-y^2}$ orbital that predominantly drives the bonding interaction, which is more evident in the NM model than the SSB-AFM model. The bonding characteristics become clearer when the electronic and crystal structures are treated in a self-consistent manner, as depicted in Figure 5(b): the bonding is significantly stronger in the NM model, while it appears markedly weaker in the SSB-AFM model. A comparison of the electron densities of the two models reveals that SSB leads to electron depletion at the center of the V-V dimer [Figure 5(c)]. This reduction is also present in the FM model [Figure 5(d)], which suggests that the principal mechanism at play is the spin-symmetry breaking, consistent with the bond overestimation in both the AFM and FM models [Figure 2(a)]. The electron depletion at the bond center diminishes the interactions between the $d_{x^2-y^2}$ orbitals, which is evident in the band structures where the $d_{x^2-y^2}$ orbital's bandwidth narrows from 0.54 eV in the spin-restricted calculation to 0.46 eV in the SSB-AFM scenario.

The ionic term present in the spin-singlet state can provide insights into the false stability of the FM spin configuration, as observed in the PBE and r²SCAN simulations [Figure 2(c)]. The FM configuration also represents a broken spin symmetry, being one of the three spin-triplet states described by:

$$\Psi_{\text{MOT,IE}}^{Triplet} = \frac{1}{2\sqrt{1-S_{1,2}}} [\varphi_2(\mathbf{r}_1)\varphi_1(\mathbf{r}_2) - \varphi_1(\mathbf{r}_1)\varphi_2(\mathbf{r}_2)] \chi_{sym} , \qquad (4)$$

where χ_{sym} is the triplet symmetric spin function. It is important to note that $\Psi_{\text{MOT,IE}}^{Triplet}$ does not incorporate any additional contribution from the ionic states, unlike $\Psi_{\text{MOT,IE}}^{Singlet}$. Therefore, when calculating the expectation value of a V-V dimer using $\Psi_{\text{MOT,IE}}^{Singlet}$ and $\Psi_{\text{MOT,IE}}^{Triplet}$ wave functions, the latter's energy is likely lower [62].

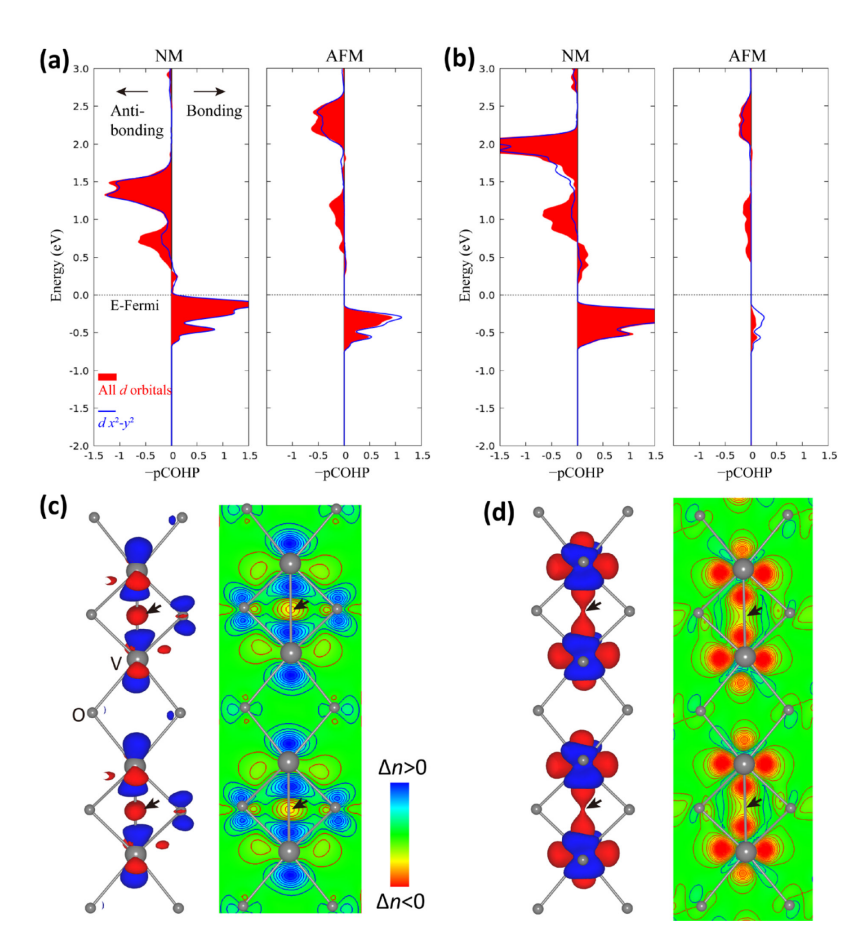


Figure 5. Chemical bonding properties of the spin-restricted NM and SSB models. (a) Diagrams of –pCOHP, showing bonding interactions between two V-V atoms within a dimer. The calculation is done with the experimental crystal structure. (b) The same as subplot (a), except for optimized geometries. (c) Electron density difference of $\Delta n = n^{\rm AFM} - n^{\rm NM}$. The experimental crystal structure is used for both states. Note the electron depletion at the V-V dimer center, denoted by black arrows. The right panel is the 2D plot of the Δn . (d) Electron density difference of $\Delta n = n^{\rm FM} - n^{\rm NM}$.

For a comprehensive understanding, it's worth mentioning another theory that was developed early on to address spin interactions in chemical bonds. This theory, known as the valence-bond theory (VBT), was developed by Heitler, London, Pauling, and Slater during the 1916-1920s [63,64,65]. The VBT and MOT were considered "rival" theories, but many theoreticians now agree that they complement each other [66,67,68]. In the Heitler-London (HL) limit, the VBT defines the singlet state wave function as [62]:

$$\Psi_{\text{VBT,HL}}^{Singlet} = \frac{1}{2\sqrt{1+S_{1,2}}} [\varphi_1(\mathbf{r}_1)\varphi_2(\mathbf{r}_2) + \varphi_2(\mathbf{r}_1)\varphi_1(\mathbf{r}_2)] [\alpha_1\beta_2 - \beta_1\alpha_2] . \tag{5}$$

It's important to note the absence of the ionic term in the HL representation. The HL treatment emphasizes the overlap of atomic orbitals in forming the valence-bond state, which increases the likelihood of electrons residing in the bond center. It is widely understood that the IE and HL wave functions are approximate representations, and the actual electronic state is likely between these extremes. In the case of M_1 VO₂, cluster dynamical mean-field theory, in conjunction with the DFT scheme (DFT+cDMFT) [69,70,71], suggested that the V-V dimer is close to the HL limit [70]. However, the inherently localized nature of the 3*d* electrons, and thus less orbital overlaps, may somewhat invalidate the HL representation for M_1 VO₂.

3.4. Spin-symmetry-breaking in the intermediate M2 VO2: An imperfect yet valuable approach

Finally, we present a situation in which SSB is highly advantageous, even though imperfect. In addition to the well-known M_1 and R phases, VO_2 can also form an intermediate phase under pressure or chemical doping conditions. Half of the V atoms form dimer chains in this phase, while the remaining V atoms are evenly dispersed. Experimentally, $M_2 VO_2$ is an insulator [21].

Figure 6 demonstrates the band structures calculated using the spin-restricted NM and SSB-AFM models, producing a metallic and an insulating phase, respectively. By projecting the orbital characters onto the band structure, we can distinguish the varying behaviors of the dimerized and non-dimerized V atoms. In the NM model, the dimerized V atoms do not contribute electrons at the Fermi level, while the non-dimerized V atoms account for the metallic nature. This metallic character arises due to the suppression of the Mott gapping mechanism as a result of the spin restriction. Conversely, in the SSB model, both the dimerized and non-dimerized V atoms can establish gaps via the Mott mechanism. It is important to acknowledge that, based on the discussion in previous sections, these two types of V atoms should ideally rely on different gapping mechanisms. Therefore, within the Kohn-Sham DFT framework, SSB is a valuable method for producing an insulating band structure of M₂ VO₂.

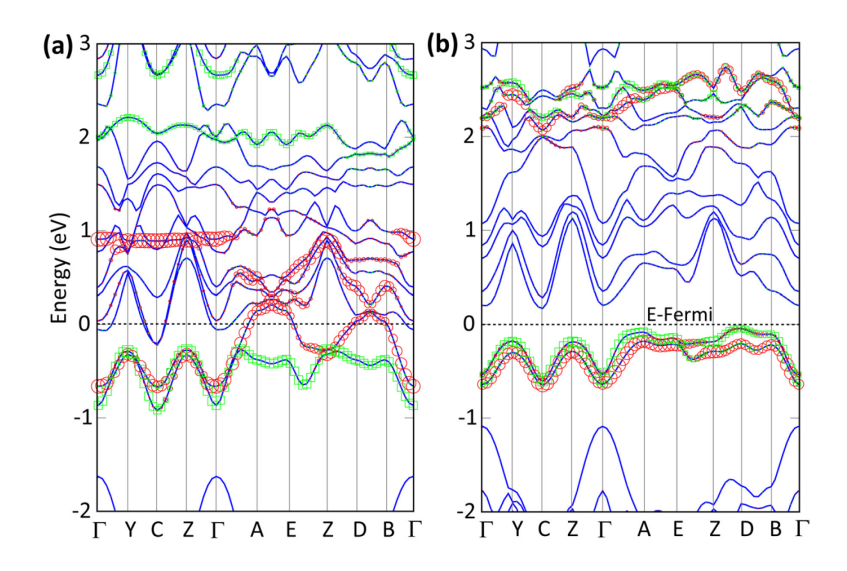


Figure 6. Band structure of M₂ VO₂. (a) Spin-restricted NM model. (b) SSB-AFM model. The red circles (green squares) represent V $d_{x^2-y^2}$ orbitals of the non-dimerized (dimerized) chain.

4. Summary

This study addresses a fundamental difficulty in characterizing the dimer structure of M_1 VO₂, primarily utilizing the advanced r^2 SCAN density functional. The metal-metal singlet state is marked by robust covalent bonding and intense spin fluctuations within a V-V dimer. However, there is a high degree of localization of V-3d electrons around equilibrium atomic positions in VO₂, which is different in the involved orbitals from the stretched H_2 molecule.

These aspects present a significant challenge to Kohn-Sham DFT methods. On one hand, the spin-restricted model severely inhibits the localization of the V-3*d* electron, which results in an unfavored high energy. The predicted dimer length is strongly underestimated. On the other hand, the SSB model respects the electron localization and thus provides a more accurate description of the electronic correlation energy. However, the predicted dimer length tends to be too long due to the excessively strong electronic repulsions, as seen in the ionic

term when presenting the two-electron wave function within the molecular-orbital theory framework. The spin-restricted and SSB models represent two extreme scenarios, with the actual V-V bonding likely existing somewhere in between.

For the ground-state total energy, the inadequacies of the Kohn-Sham determinant as an approximation to the true wavefunction should (except in special cases, including failure of the exact density to be non-interacting v-representable) be exactly compensated by the sum of the Hartree energy and the exact density functional for the exchange-correlation energy. But we only have approximate functionals, which compensate imperfectly. R^2SCAN was constructed to respect most known mathematical properties of the exact functional, but none of the functionals tested here is exact for all one-electron densities. Thus, VO_2 stands as a challenge to any self-interaction correction to r^2SCAN that exists (e.g., the +U correction [30] or the full Fermi-Löwdin self-interaction correction [72] or an improved self- interaction correction to be developed.)

These findings highlight the continuing challenges faced by the DFT approaches in accurately describing the metal-metal singlet bonding. A reliable treatment should allow for breaking the spin-symmetry while capturing intense spin interactions more accurately. Currently, the combination of r^2SCAN with SSB is an imperfect yet valuable approach, as demonstrated in the intermediate M_2 VO₂ phase. Our results on VO₂ also have broader implications for calculations of quantum antiferromagnets in general, such as quantum spin liquid systems.

Acknowledgments

We thank Youjin Deng, Peihong Zhang, and Yuanyao He for their fruitful discussions. YZ and DK are supported by the Fujian Natural Science Foundation (2023J02032), Guangdong Natural Science Foundation (2021A1515010049), and the National Natural Science Foundation of China (11904156). The work of JPP was supported by the U.S. National Science Foundation under Grant No. DMR-1939528, and by the U.S. Department of Energy. Basic Energy Sciences, under Grant. No. DE-SC18331. J.S. acknowledges the support of the U.S. Office of Naval Research (ONR) Grant No. N00014-22-1-2673.

References

- [1] Daniel Khomskii, Transition metal compounds. 2014: Cambridge University Press.
- [2] W. Kohn, L. J. Sham, *Self-Consistent Equations Including Exchange and Correlation Effects*. Phys. Rev. 140, A1133 (1965).
- [3] Nevill Mott, Metal-insulator transitions. 2004: CRC Press.
- [4] P. Hohenberg, W. Kohn, Inhomogeneous Electron Gas. Phys. Rev. 136, B864 (1964).
- [5] Jianwei Sun, Adrienn Ruzsinszky, John P Perdew, *Strongly Constrained and Appropriately Normed Semilocal Density Functional*. Phys. Rev. Lett. 115, 036402 (2015).
- [6] John P. Perdew, Adrienn Ruzsinszky, Jianwei Sun, Niraj K. Nepal, Aaron D. Kaplan, *Interpretations of ground-state symmetry breaking and strong correlation in wavefunction and density functional theories*. Proc. Natl. Acad. Sci. U.S.A. 118, e2017850118 (2021).
- [7] Yubo Zhang, James Furness, Ruiqi Zhang, Zhi Wang, Alex Zunger, Jianwei Sun, *Symmetry-breaking polymorphous descriptions for correlated materials without interelectronic U.* Phys. Rev. B. 102, 045112 (2020).
- [8] James W. Furness, Yubo Zhang, Christopher Lane, Ioana Gianina Buda, Bernardo Barbiellini, Robert S. Markiewicz, Arun Bansil, Jianwei Sun, *An accurate first-principles treatment of doping-dependent electronic structure of high-temperature cuprate superconductors.* Communications Physics. 1, 11 (2018).

- [9] Yubo Zhang, Christopher Lane, James W. Furness, Bernardo Barbiellini, John P. Perdew, Robert S. Markiewicz, Arun Bansil, Jianwei Sun, *Competing stripe and magnetic phases in the cuprates from first principles*. Proc. Natl. Acad. Sci. U.S.A. 117, 68 (2020).
- [10] P. W. Anderson, More Is Different. Science. 177, 393 (1972).
- [11] Richard M Martin, Lucia Reining, David M Ceperley, Interacting electrons. 2016: Cambridge University Press.
- [12] S. V. Streltsov, D. I. Khomskii, *Orbital physics in transition metal compounds: new trends.* Physics-Uspekhi. 60, 1121 (2017).
- [13] Daniel I. Khomskii, Sergey V. Streltsov, *Orbital Effects in Solids: Basics, Recent Progress, and Opportunities*. Chem. Rev. 121, 2992 (2021).
- [14] D. I. Khomskii, *Review—Orbital Physics: Glorious Past, Bright Future*. ECS J. Solid State Sci. Technol. 11, 054004 (2022).
- [15] H. F. Pen, J. van den Brink, D. I. Khomskii, G. A. Sawatzky, *Orbital Ordering in a Two-Dimensional Triangular Lattice*. Phys. Rev. Lett. 78, 1323 (1997).
- [16] V. Eyert, The metal-insulator transitions of VO2: A band theoretical approach. Ann. Phys. 514, 650 (2002).
- [17] Takaaki Jin-no, Yasuhiro Shimizu, Masayuki Itoh, Seiji Niitaka, Hidenori Takagi, *Orbital reformation with vanadium trimerization in d*² *triangular lattice LiVO*₂ *revealed by* ⁵¹*V NMR*. Phys. Rev. B. 87, 075135 (2013).
- [18] E. SÁNdor, W. A. Wooster, Extra Streaks in the X-ray Diffraction Pattern of Vanadium Single Crystals. Nature. 182, 1435 (1958).
- [19] Sergey V. Streltsov, Daniel I. Khomskii, *Covalent bonds against magnetism in transition metal compounds*. Proc. Natl. Acad. Sci. U.S.A. 113, 10491 (2016).
- [20] John P. Perdew, Karla Schmidt, *Jacob's ladder of density functional approximations for the exchange-correlation energy.* AIP Conf. Proc. 577, 1 (2001).
- [21] Jean-Paul Pouget, *Basic aspects of the metal–insulator transition in vanadium dioxide VO2: a critical review.* Comptes Rendus. Physique. 22, 37 (2021).
- [22] John B. Goodenough, *The two components of the crystallographic transition in VO2*. J. Solid State Chem. 3, 490 (1971).
- [23] Mel Levy, Universal variational functionals of electron densities, first-order density matrices, and natural spin-orbitals and solution of the v-representability problem. Proc. Natl. Acad. Sci. U.S.A. 76, 6062 (1979).
- [24] Aaron D. Kaplan, Mel Levy, John P. Perdew, *The Predictive Power of Exact Constraints and Appropriate Norms in Density Functional Theory.* Annu. Rev. Phys. Chem. 74, 193 (2023).
- [25] O. Gunnarsson, B. I. Lundqvist, *Exchange and correlation in atoms, molecules, and solids by the spin-density-functional formalism.* Phys. Rev. B. 13, 4274 (1976).
- [26] John P. Perdew, Shah Tanvir ur Rahman Chowdhury, Chandra Shahi, Aaron D. Kaplan, Duo Song, Eric J. Bylaska, Symmetry Breaking with the SCAN Density Functional Describes Strong Correlation in the Singlet Carbon Dimer. J. Phys. Chem. A. 127, 384 (2023).
- [27] Chen Li, Xiao Zheng, Neil Qiang Su, Weitao Yang, Localized orbital scaling correction for systematic elimination of delocalization error in density functional approximations. National Science Review. 5, 203 (2017).
- [28] J. P. Perdew, Alex Zunger, *Self-interaction correction to density-functional approximations for many-electron systems*. Phys. Rev. B. 23, 5048 (1981).
- [29] Rajendra R. Zope, Yoh Yamamoto, Carlos M. Diaz, Tunna Baruah, Juan E. Peralta, Koblar A. Jackson, Biswajit Santra, John P. Perdew, *A step in the direction of resolving the paradox of Perdew-Zunger self-interaction correction*. J. Chem. Phys. 151, (2019).
- [30] Matteo Cococcioni, Stefano de Gironcoli, *Linear response approach to the calculation of the effective interaction parameters in the LDA+U method.* Phys. Rev. B. 71, 035105 (2005).

- [31] I. A. Misurkin, A. A. Ovchinnikov, *Antiferromagnetic spin structure of long molecules with conjugated bonds*. Mol. Phys. 27, 237 (1974).
- [32] D. C. Langreth, J. P. Perdew, *The exchange-correlation energy of a metallic surface*. Solid State Commun. 17, 1425 (1975).
- [33] John P. Perdew, Kieron Burke, Matthias Ernzerhof, *Generalized Gradient Approximation Made Simple*. Phys. Rev. Lett. 77, 3865 (1996).
- [34] John P. Perdew, Kieron Burke, Yue Wang, *Generalized gradient approximation for the exchange-correlation hole of a many-electron system.* Phys. Rev. B. 54, 16533 (1996).
- [35] John P. Perdew, Matthias Ernzerhof, Kieron Burke, Andreas Savin, *On-top pair-density interpretation of spin density functional theory, with applications to magnetism.* Int. J. Quantum Chem. 61, 197 (1997).
- [36] James W. Furness, Aaron D. Kaplan, Jinliang Ning, John P. Perdew, Jianwei Sun, *Accurate and Numerically Efficient r2SCAN Meta-Generalized Gradient Approximation*. J. Phys. Chem. Lett. 11, 8208 (2020).
- [37] G. Kresse, J. Furthmüller, *Efficiency of ab-initio total energy calculations for metals and semiconductors using a plane-wave basis set.* Comput. Mater. Sci. 6, 15 (1996).
- [38] G. Kresse, J. Furthmüller, *Efficient iterative schemes for ab initio total-energy calculations using a plane-wave basis set.* Phys. Rev. B. 54, 11169 (1996).
- [39] Joachim Paier, Martijn Marsman, K Hummer, Georg Kresse, Iann C Gerber, János G Ángyán, *Screened hybrid density functionals applied to solids*. J. Chem. Phys. 124, 154709 (2006).
- [40] Jochen Heyd, Gustavo E Scuseria, Matthias Ernzerhof, *Hybrid functionals based on a screened Coulomb potential*. J. Chem. Phys. 118, 8207 (2003).
- [41] A. I. Liechtenstein, M. I. Katsnelson, V. P. Antropov, V. A. Gubanov, *Local spin density functional approach to the theory of exchange interactions in ferromagnetic metals and alloys.* J. Magn. Magn. Mater. 67, 65 (1987).
- [42] Xu He, Nicole Helbig, Matthieu J. Verstraete, Eric Bousquet, *TB2J: A python package for computing magnetic interaction parameters*. Comput. Phys. Commun. 264, 107938 (2021).
- [43] Richard Dronskowski, Peter E. Bloechl, *Crystal orbital Hamilton populations (COHP): energy-resolved visualization of chemical bonding in solids based on density-functional calculations.* J. Phys. Chem. 97, 8617 (1993).
- [44] Volker L. Deringer, Andrei L. Tchougréeff, Richard Dronskowski, *Crystal Orbital Hamilton Population (COHP) Analysis As Projected from Plane-Wave Basis Sets.* J. Phys. Chem. A. 115, 5461 (2011).
- [45] Stefan Maintz, Volker L. Deringer, Andrei L. Tchougréeff, Richard Dronskowski, *LOBSTER: A tool to extract chemical bonding from plane-wave based DFT.* J. Comput. Chem. 37, 1030 (2016).
- [46] Rudolf Peierls, More surprises in theoretical physics. 1991: Princeton University Press.
- [47] Jianwei Sun, Richard C. Remsing, Yubo Zhang, Zhaoru Sun, Adrienn Ruzsinszky, Haowei Peng, Zenghui Yang, Arpita Paul, Umesh Waghmare, Xifan Wu, Michael L. Klein, John P. Perdew, *Accurate first-principles structures and energies of diversely bonded systems from an efficient density functional*. Nature Chemistry. 8, 831 (2016).
- [48] Yubo Zhang, Jianwei Sun, John P. Perdew, Xifan Wu, *Comparative first-principles studies of prototypical ferroelectric materials by LDA, GGA, and SCAN meta-GGA*. Phys. Rev. B. 96, 035143 (2017).
- [49] Yubo Zhang, Daniil A. Kitchaev, Julia Yang, Tina Chen, Stephen T. Dacek, Rafael A. Sarmiento-Pérez, Maguel A. L. Marques, Haowei Peng, Gerbrand Ceder, John P. Perdew, Jianwei Sun, *Efficient first-principles prediction of solid stability: Towards chemical accuracy.* npj Computational Materials. 4, 9 (2018).
- [50] Yubo Zhang, James W. Furness, Bing Xiao, Jianwei Sun, Subtlety of TiO2 phase stability: Reliability of the density functional theory predictions and persistence of the self-interaction error. J. Chem. Phys. 150, 014105 (2019).
- [51] N. Read, Subir Sachdev, Spin-Peierls, valence-bond solid, and Neel ground states of low-dimensional quantum antiferromagnets. Phys. Rev. B. 42, 4568 (1990).
- [52] N. Read, Subir Sachdev, Valence-bond and spin-Peierls ground states of low-dimensional quantum

- antiferromagnets. Phys. Rev. Lett. 62, 1694 (1989).
- [53] A. Liebsch, H. Ishida, G. Bihlmayer, *Coulomb correlations and orbital polarization in the metal-insulator transition of VO2*. Phys. Rev. B. 71, 085109 (2005).
- [54] Subir Sachdev, The quantum phases of matter. arXiv:1203.4565, (2012).
- [55] Ch Rüegg, B. Normand, M. Matsumoto, A. Furrer, D. F. McMorrow, K. W. Krämer, H. U. Güdel, S. N. Gvasaliya, H. Mutka, M. Boehm, *Quantum Magnets under Pressure: Controlling Elementary Excitations in TlCuCl3*. Phys. Rev. Lett. 100, 205701 (2008).
- [56] G. Bastien, G. Garbarino, R. Yadav, F. J. Martinez-Casado, R. Beltrán Rodríguez, Q. Stahl, M. Kusch, S. P. Limandri, R. Ray, P. Lampen-Kelley, D. G. Mandrus, S. E. Nagler, M. Roslova, A. Isaeva, T. Doert, L. Hozoi, A. U. B. Wolter, B. Büchner, J. Geck, J. van den Brink, *Pressure-induced dimerization and valence bond crystal formation in the Kitaev-Heisenberg magnet RuCl3*. Phys. Rev. B. 97, 241108 (2018).
- [57] Robert S. Mulliken, The Assignment of Quantum Numbers for Electrons in Molecules. I. Phys. Rev. 32, 186 (1928).
- [58] Robert S. Mulliken, *The Assignment of Quantum Numbers for Electrons in Molecules. II. Correlation of Molecular and Atomic Electron States.* Phys. Rev. 32, 761 (1928).
- [59] Robert S. Mulliken, *The Assignment of Quantum Numbers for Electrons in Molecules. III. Diatomic Hydrides.* Phys. Rev. 33, 730 (1929).
- [60] F. Hund, Zur Deutung der Molekelspektren. IV. Z. Phys. 51, 759 (1928).
- [61] F. Hund, Zur Frage der chemischen Bindung. Z. Phys. 73, 1 (1932).
- [62] Joachim Stöhr, Hans Christoph Siegmann, *Magnetism From fundamentals to nanoscale dynamics*. Vol. 5. 2006: Springer, Berlin, Heidelberg. 236.
- [63] Gilbert N. Lewis, THE ATOM AND THE MOLECULE. J. Am. Chem. Soc. 38, 762 (1916).
- [64] Linus Pauling, The nature of the chemical bond. 3 ed. 1939: Cornell University Press.
- [65] W. Heitler, F. London, *Wechselwirkung neutraler Atome und homöopolare Bindung nach der Quantenmechanik.* Z. Phys. 44, 455 (1927).
- [66] John Morrison Galbraith, Sason Shaik, David Danovich, Benoît Braïda, Wei Wu, Philippe Hiberty, David L. Cooper, Peter B. Karadakov, Thom H. Dunning, Jr., Valence Bond and Molecular Orbital: Two Powerful Theories that Nicely Complement One Another. J. Chem. Educ. 98, 3617 (2021).
- [67] Sason Shaik, David Danovich, Philippe C. Hiberty, *Valence Bond Theory—Its Birth, Struggles with Molecular Orbital Theory, Its Present State and Future Prospects.* Molecules. 26, 1624 (2021).
- [68] Gernot Frenking, Sason Shaik, *The chemical bond: fundamental aspects of chemical bonding*. Vol. 1. 2014: John Wiley & Sons.
- [69] W. H. Brito, M. C. O. Aguiar, K. Haule, G. Kotliar, *Dynamic electronic correlation effects in NbO2 as compared to VO2.* Phys. Rev. B. 96, 195102 (2017).
- [70] S. Biermann, A. Poteryaev, A. I. Lichtenstein, A. Georges, *Dynamical Singlets and Correlation-Assisted Peierls Transition in VO2*. Phys. Rev. Lett. 94, 026404 (2005).
- [71] Bence Lazarovits, Kyoo Kim, Kristjan Haule, Gabriel Kotliar, *Effects of strain on the electronic structure of VO₂*. Phys. Rev. B. 81, 115117 (2010).
- [72] Mark R. Pederson, Adrienn Ruzsinszky, John P. Perdew, *Communication: Self-interaction correction with unitary invariance in density functional theory.* J. Chem. Phys. 140, 121103 (2014).